

# Anisotropy dispersion effects on the high frequency behavior of soft magnetic Fe–Co–N thin films

N. X. Sun<sup>a)</sup> and S. X. Wang

Center of Research on Information Storage Materials (CRISM), and Geballe Laboratory of Advanced Materials, Stanford University, Stanford, California 94305-4045

(Presented on 12 November 2002)

The high frequency behavior beyond 1 GHz of a Fe–Co–N film and a NiFe/Fe–Co–N film [NiFe stands for Ni<sub>81</sub>Fe<sub>19</sub>(wt. %)], shown as promising magnetic write head materials previously, has been investigated using a pulse inductive microwave magnetometer in this work. The NiFe/Fe–Co–N film, which has a smaller dispersion angle ( $\sim 0.8^\circ$ ) than the Fe–Co–N film ( $\sim 2^\circ$ ), shows a smaller damping parameter and a higher ferromagnetic resonance frequency when longitudinally biased. When the Fe–Co–N film is transversely biased, the damping parameter of the Fe–Co–N film shows a diffuse peak at a transverse field of 1.76 kA/m (22 Oe), and its ferromagnetic resonance frequency shows a small local maximum at 1.76 kA/m (22 Oe). In contrast, the damping parameter of the NiFe/Fe–Co–N film shows a sharp peak at a transverse field of 1.4 kA/m (18 Oe), and its ferromagnetic resonance frequency displays a sharp local maximum also at a transverse field of 1.4 kA/m (18 Oe) too, which is very close to the dc anisotropy field. The sharp peak in the ferromagnetic resonance frequency and the damping parameter of the NiFe/Fe–Co–N film is due to the generation of a higher order (very close to the second order) ferromagnetic absorption when the ac field is large compared to the net in-plane dc magnetic field. © 2003 American Institute of Physics. [DOI: 10.1063/1.1557347]

Coherent rotation of magnetization is desired for real applications of magnetic films such as magnetic recording heads and microinductors, since it corresponds to a fast switching of the magnetization. In real soft magnetic films, due to the local variation of the anisotropy axes over the whole film area, coherent rotation will only occur when the angle between the applied field and the hard axis is less than  $(90^\circ - \alpha)$  at low frequencies.<sup>1</sup> The dispersion angle  $\alpha$  can be estimated by a standard  $B$ – $H$  loop, and is typically less than  $1^\circ$  for soft magnetic films with a good uniaxial anisotropy. How the dispersion angle affects the high frequency behavior is still not well understood and under intensive research.

Fe–Co–N films with the thickness of 100 nm with NiFe (Ni<sub>81</sub>Fe<sub>19</sub>(wt. %)) nanounderlayer (<5 nm) have been synthesized with a high saturation magnetization of  $\mu_0 M_s = 2.4$  T, an anisotropy field of about 1.6 kA/m (20 Oe), and a low coercivity of less than 80 A/m (1 Oe).<sup>2,3</sup> The Fe–Co–N films show a high initial permeability of 1000 with a bandwidth of 1.5 GHz. The dispersion angles  $\alpha_{50}$  of the NiFe/Fe–Co–N films can be tuned by changing the Permalloy underlayer thickness, being  $2^\circ$  for the Fe–Co–N single layer film, and  $0.8^\circ$  for the NiFe/Fe–Co–N film with a Permalloy underlayer thickness of 2.5 nm.<sup>4</sup> The Fe–Co–N single layer and the NiFe/Fe–Co–N film serve as excellent model specimen for studying the dispersion angle effects on the high frequency behavior of magnetic films due to their drastic difference in dispersion angle, but similarity in other properties like saturation magnetization and anisotropy field.

In this work, the high frequency behavior of the Fe–Co–N single layer film and the NiFe/Fe–Co–N film is studied and compared.

Fe–Co–N films were deposited onto 0.5 mm thick Si wafers with a resistivity of 10–20  $\Omega$  cm through reactive rf diode sputtering in an argon and nitrogen atmosphere. The target composition was Fe<sub>70</sub>Co<sub>30</sub>(at.%) with a purity of 99.95%. The Permalloy underlayer was deposited in a pure argon atmosphere by rf sputtering with a target composition of Ni<sub>81</sub>Fe<sub>19</sub>(wt. %). The base pressure of the sputtering chamber was  $\sim 2.7 \times 10^{-5}$  Pa ( $2 \times 10^{-7}$  Torr). Magnetic properties of the NiFe/Fe–Co–N films were characterized by a  $B$ – $H$  loop. The dispersion angles of magnetic films were measured on a standard  $B$ – $H$  loop.<sup>1</sup> A pulsed inductive microwave magnetometer (PIMM)<sup>5</sup> was used to study the high frequency behavior of the NiFe/Fe–Co–N films. In this work, the amplitude of the step magnetic field is chosen to be about 200 A/m (2.5 Oe), which is much smaller than the anisotropy field of 1.6 kA/m (20 Oe). The magnetization oscillates with an angular amplitude of less than 130 mrad under such an excitation field, satisfying the small-signal condition.

The PIMM signals from the Fe–Co–N single layer film and the NiFe/Fe–Co–N show the typical exponentially decreasing sinusoidal curves. The Landau–Lifshitz damping constants are obtained from the time domain curves and shown in Fig. 1 as a function of the longitudinal bias field. The NiFe/Fe–Co–N film with a low dispersion angle  $\alpha_{50}$  of  $0.8^\circ$  shows a much lower damping constant compared to the Fe–Co–N single layer film with a dispersion angle  $\alpha_{50}$  of  $2^\circ$  at all bias fields. At zero longitudinal bias field, the NiFe/Fe–Co–N film shows a damping parameter of 0.019; while Fe–

<sup>a)</sup>Currently at IBM Storage Technology Division, San Jose, CA 95193; electronic mail: nxsun@us.ibm.com

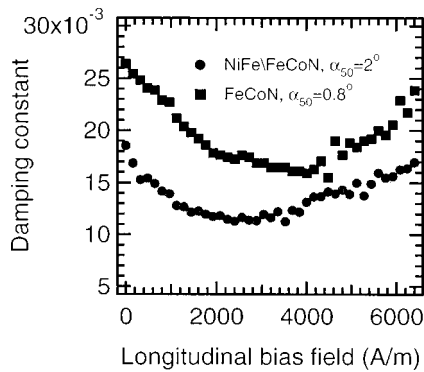


FIG. 1. Damping constant for the Fe–Co–N film (squares) and a NiFe/Fe–Co–N film (circles).

Co–N film shows a much larger damping parameter of 0.027. The damping constants drop with the bias fields at low bias fields, but increase with the longitudinal bias field when the bias field is larger than 3.2 kA/m (40 Oe). It is notable that all the damping constants in Fig. 1 are in the range of 0.01–0.03.

The time domain PIMM data were transformed into the frequency domain to get the ferromagnetic resonance (FMR) frequencies. Two types of FMR frequencies were recorded: the FMR frequency, or the peak frequency of the imaginary permeability, and the zero-cross FMR frequency, the frequency at which the real part of the permeability drops to zero. The FMR frequencies are shown in Fig. 2 as a function of the longitudinal bias field for both the Fe–Co–N film and the NiFe/Fe–Co–N film. The FMR frequencies increase continuously with the longitudinal bias field due to the increase of the net magnetic field in the film when longitudinally biased. Clearly the NiFe/Fe–Co–N film with a dispersion angle of 0.8° shows higher FMR frequencies at all bias fields than the single layer Fe–Co–N film that has a high dispersion angle of 2°. The FMR frequency at zero bias field is 2.0 GHz for the NiFe/Fe–Co–N film, while the single layer Fe–Co–N film show a FMR frequency of 1.7 GHz at zero longitudinal bias field.

If the damping constant  $\alpha$  is taken into consideration, the FMR frequency of a magnetic film with an anisotropy field of  $H_k$  at a longitudinal bias field  $H_{\text{appl}}$  in the small signal limit can be expressed as<sup>4</sup>  $f_{\text{FMR}} = (\gamma/2\pi)\mu_0\sqrt{M_s[H_k + H_{\text{appl}} - (\alpha/2)^2 \cdot M_s]}$ , where  $\gamma$  is the

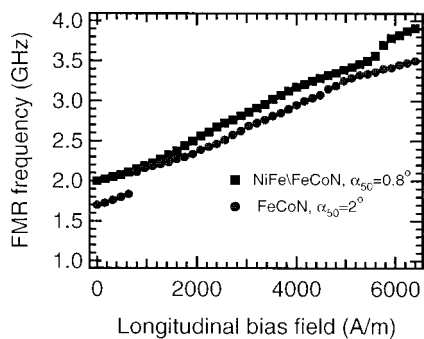


FIG. 2. Comparison of the peak FMR frequencies for the Fe–Co–N film (squares), and a NiFe/Fe–Co–N film (circles).

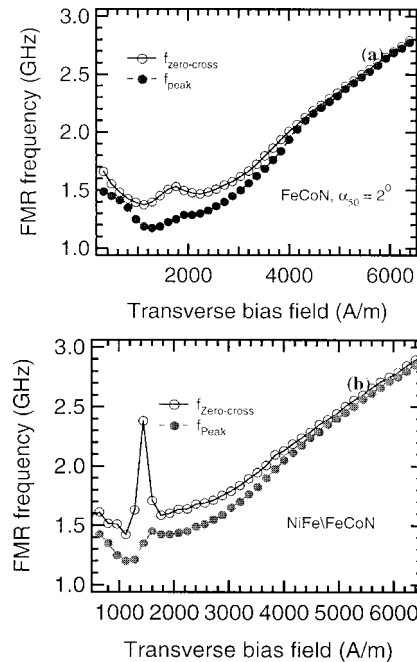


FIG. 3. Peak FMR frequency and zero-cross FMR frequency as a function of the transverse bias field for: (a) the Fe–Co–N film and (b) the NiFe/Fe–Co–N film.

gyromagnetic ratio and equal to  $2\pi \times 28 \times 10^9$  rad/(s T) and  $M_s$  is the saturation magnetization. The equation for the FMR frequency can be reduced to the Kittel equation<sup>6</sup> when  $\alpha=0$ . Clearly, a higher damping constant in the magnetic film results in a lower FMR frequency and in turn a narrower bandwidth. Accordingly, when the magnetic film is critically damped, which is  $\alpha_{\text{cri}} = 2/\sqrt{\chi_0} = 0.058$  for the Fe–Co–N films with the initial susceptibility  $\chi_0$  of 1200,<sup>4</sup> the FMR frequency will be reduced to zero. Clearly, the damping constants are not negligibly small in the Fe–Co–N film with a damping constant of 0.027, which is nearly half of the critical damping constant. For the Fe–Co–N film and the NiFe/Fe–Co–N film with very similar values for  $M_s$ , the anisotropy field and the damping constant are the only parameters that can change the FMR frequency, according to the Kittel equation. The  $H_k$  value extrapolated from the FMR frequencies for the NiFe/Fe–Co–N film is 1.6 kA/m (20 Oe) at low bias fields and 1.28 kA/m (16 Oe) at large bias fields.<sup>4</sup> By assuming a  $\mu_0 M_s$  of 2.4 T and an  $H_k$  of 1.6 kA/m (20 Oe) for both films, the peak FMR frequency at zero bias fields determined by the above equation is 1.84 and 1.71 GHz for the NiFe/Fe–Co–N and the Fe–Co–N film, respectively. The calculated FMR frequency for the NiFe/Fe–Co–N film is lower than the measured value; while the measured and calculated FMR values for the Fe–Co–N film correspond well with each other.

Similar to what is done for the longitudinally biased impulse responses, the transversely biased impulse responses are obtained and analyzed. The peak FMR frequency and the zero-cross FMR frequency for the Fe–Co–N film with a dispersion angle of  $\alpha_{50}$  of 2° are shown in Fig. 3(a). The peak FMR frequency first drops from 1.5 GHz to a minimum of 1.2 GHz at a transverse bias field of 1.28 kA/m (16 Oe), then

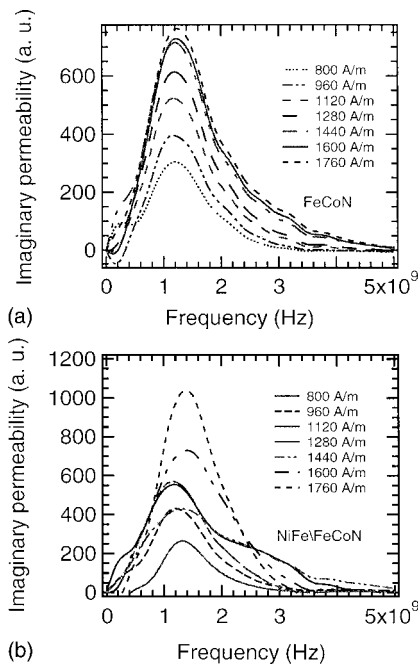


FIG. 4. Imaginary permeability spectra of: (a) the Fe–Co–N film and (b) NiFe/Fe–Co–N film at different transverse bias fields.

it increases steadily up to 2.8 GHz at a transverse bias of 6.4 kA/m (80 Oe). The zero-cross FMR frequency of the single layer Fe–Co–N film shows a small broad local maximum at a transverse bias field of 1.76 kA/m (22 Oe), and then the zero-cross FMR frequency increases with the increment of transverse bias field. The zero-cross FMR frequency for the NiFe/Fe–Co–N film with a dispersion angle of  $\alpha_{50}$  of  $0.8^\circ$ , however, shows a very sharp local maximum value of 2.4 GHz when the transverse bias field is at 18 Oe as shown in Fig. 3(b), while no peaking is observed in the peak FMR frequency. The imaginary spectra for the Fe–Co–N single layer always show a single peak at different transverse bias fields, as indicated in Fig. 4(a). The imaginary permeability

spectra for the NiFe/Fe–Co–N film, however, show different features at different bias fields as indicated in Fig. 4(b). When the transverse bias field is lower than 1.28 kA/m (16 Oe), there is always a single peak in the imaginary spectra; while when the bias field is at 1.28 kA/m (16 Oe) and 1.44 kA/m (18 Oe), a clear shoulder on the big absorption peak of the imaginary spectrum appears. The imaginary spectrum is broadened by the shoulder, which corresponds to a large damping parameter, as shown in Fig. 3(b). This big shoulder in the imaginary spectra also causes a large shift in the zero-cross frequency by changing the real permeability spectrum. The big shoulder in the imaginary permeability can be decomposed into a superposition of two peaks, the first peak and the second peak, and has a peak frequency very close to twice the first peak, which has an area of over 30% of the first peak. The second peak only appears when the transverse external magnetic field nearly compensates the uniaxial anisotropy of the film, resulting in a relatively large susceptibility. The large amplitude of magnetization motion is possibly a source of nonlinear magnetization dynamics.<sup>7</sup> More work is needed to identify the origin of the higher order absorption.

Assistance on this work from Dr. Tom Silva and Tony Kos at NIST is gratefully acknowledged. The authors would like to thank Dr. Carl Patton for helpful discussions. This work is supported in part by NSF under Grant Nos. ECS-9710223 and ECS-0096704.

<sup>1</sup>W. R. Beam and K. Y. Ahn, J. Appl. Phys. **34**, 1561 (1963).

<sup>2</sup>S. X. Wang, N. X. Sun, M. Yamaguchi, and S. Yabukami, Nature (London) **407**, 150 (2000).

<sup>3</sup>N. X. Sun and S. X. Wang, IEEE Trans. Magn. **36**, 2506 (2000).

<sup>4</sup>N. X. Sun, S. X. Wang, T. J. Silva, and A. B. Kos, IEEE Trans. Magn. **38**, 146 (2002).

<sup>5</sup>T. J. Silva, C. S. Lee, T. M. Crawford, and C. T. Rogers, J. Appl. Phys. **86**, 7849 (1999).

<sup>6</sup>C. Kittel, *Introduction to Solid State Physics*, 7th ed. (Wiley, New York, 1996), p. 505.

<sup>7</sup>A. G. Gurevich and G. A. Melkov, *Magnetization Oscillations and Waves* (Chemical Rubber, Boca Raton, FL, 1996), p. 231.